https://doi.org/10.1016/j.cej.2020.128313

Self-protonating, plasma polymerized, superimposed multi-layered biomolecule nanoreservoir as blood-contacting surfaces

Wenxuan Wang[1], Lei Lu[1,2] Ho Pan Bei[3], Xiangyang Li[1], Zeyu Du[1], Manfred F. Maitz[4], Nan Huang[1], Qiufen Tu[1], Xin Zhao[3]*, Zhilu Yang[1]**

[1]Key Laboratory of Advanced Technologies of Materials, Ministry of Education, School of Materials Science and Engineering, Southwest Jiaotong University, Chengdu 610031, China.

[2]School of Life Science and Engineering, Southwest Jiaotong University, Chengdu 610031, China.

[3]Department of Biomedical Engineering, The Hong Kong Polytechnic University, Hung Hom, Kowloon, Hong Kong, China

[4]Max Bergmann Center of Biomaterials, Leibniz Institute of Polymer Research Dresden, Dresden 01069, Germany

Email: tuqiufen@home.swjtu.edu.cn; xin.zhao@polyu.edu.hk; zhiluyang1029@swjtu.edu.cn

Keywords: Self-protonation, Plasma polymerization, Biomolecule nanoreservoir, Blood contacting surface

Abstract

Blood-contacting devices have emerged in the 21st century as the go-to clinical treatment for severe cardiovascular diseases. Due to their poor hemocompatibility, many coatings have been developed to improve their biocompatibility with limited success due to the lack of robustness in biomolecule conjugation. In this work, we propose a new self-protonating, plasma polymerized, superimposed multi-layered nanoreservoir coating for immobilization of charged biomolecules, and demonstrated its high surface charge density, loading capabilities and most importantly, bioactivity retention of biomolecules. Using heparin as a model therapeutic, we demonstrated the advantages of our coating strategy through *in vitro* and *ex vivo* means. Our findings will open a new path in clinical device coating strategies in biomolecule functionalization to benefit many patients worldwide.

Introduction

Cardiovascular diseases (CVDs) can be treated with blood-contacting devices such as artificial heart valves and stents, limited only by their biocompatibility. Upon implantation, exposure of bare devices inevitably leads to a series of complications like thrombosis caused by activation of platelets and fibrins, which gives rise to many studies of biocompatible coatings to shield the artificial material from native environments [1-3]. Covalent bonding can be used to securely functionalize these devices with biomolecules including polysaccharides and proteins. This bonding, unfortunately, takes up the essential surface reactive sites of biomolecules to perform conformational motions for a “lock-and-key” interaction, greatly hindering their bioactivity [4]. Meanwhile, non-covalent methods are able to preserve unrestricted arrangement of the affixed biomolecules, but are often less strong due to the weak electrostatic interactions. Layer-by-layer

(LbL) deposition (i.e., stacking multiple layers) allows for conjugation of biomolecules onto the coatings directly, but suffers from the multi-layer bulkiness (~1 μm) and difficulty in precise tuning of deposition parameters, limiting its clinical application [5]. Additionally, some LbL approaches require acidic conditions to initiate the conjugation process, further lowering their compatibility with biomolecules. Owing to these limitations, new methods for coating preparation such as plasma polymerization have emerged to circumvent these problems. To achieve robust biomolecule immobilization onto stainless steel stents, polymeric allylamine was plasma polymerized to create a dense coating of amine groups for click-chemistry reaction with bivalirudin [6]. Yet this method is highly specific, orientation-locked and could only be applied to molecules with viable surface reaction groups with carbodiimide. On the other hand, single-layered polypyrrole was plasma polymerized for physisorption of bovine serum albumin (BSA) molecules, but has difficulty retaining the absorbed BSAs due to the lack of protonating capability and its reliance on acidic pH to initiate protonation [7]. Henceforth, a "perfect" device coating should have good strength and nano-scale properties to resist abrasion, conserve biomolecule activity and are substantially charged for simplistic and sufficient anchoring of substrates.

Here, we introduce a novel self-protonating, plasma polymerized, superimposed multi-layered nanoreservoir coating for non-covalent but strong immobilization of large amounts of biomolecules. Using plasma polymerization, we stack acrylic acid (PPAac) and amine-bearing allylamine (PPAam) nano-layers in an alternative fashion, which acts as a thin (60 nm) but powerful battery reservoir through self-protonation and provides biomolecules with strong positive charges for adhesion even under physiological pHs **(Figure 1A)**. This plasma-polymerized, ultra-thin nanocoatings is designed to have minimal effects on lumen size for

prevention of occlusion while maintaining decent charge potency. Additionally, each alternating layer is expected to increase the redox potential difference of the coating, accumulating to a vastly superior surface charge compared to singular coatings. Traditional LbL coatings rely on positively charged H^+ ions under acidic conditions for conjugation of biomolecules, which are inevitably neutralized by the increased level of OH^- groups at physiological pHs and causes burst release of biomolecules [8]. Unlike these coatings, all of the functionalization of our coating was performed at physiological pHs, thus immobilization of biomolecules do not revert post-implantation when they were exposed back in native environments. As proof-of-concept, we chose heparin, a polysaccharide which originates from liver and is widely used in blood-contacting coatings, to demonstrate the conjugation efficacy of our system. As one of the most negatively charged biomolecules, heparin has strong affinity to the self-protonating coating and can be electrostatically immobilized under neutral pH through our unprecedented, simple one-step assembling process with excellent stability, retention of bioactivity and loading capacity (>500 ng/cm^2). In our system, biomolecule retention remains excellent under continuous washing (>95%) while heparin is shown to retain its bioactivity in preventing fibrinogen adsorption and platelet activation in both human plasma and blood circulation of rabbit *ex vivo* models. This is all achieved in a green, one-pot anchoring of biomolecules at physiological pH and temperatures, made only available through the generation of a large longitudinal updraft of protons to the surface from our densely alternating, crepe-cake like nanoreservoir coating. This novel coating strategy allows for robust application of any charged biomolecules onto implantable biomedical devices while safeguarding their bioactivity, and will open up many more opportunities at supplementing recovery from pathological or traumatic situations using more environmentally sensitive biomolecules such as growth factors and hormones.

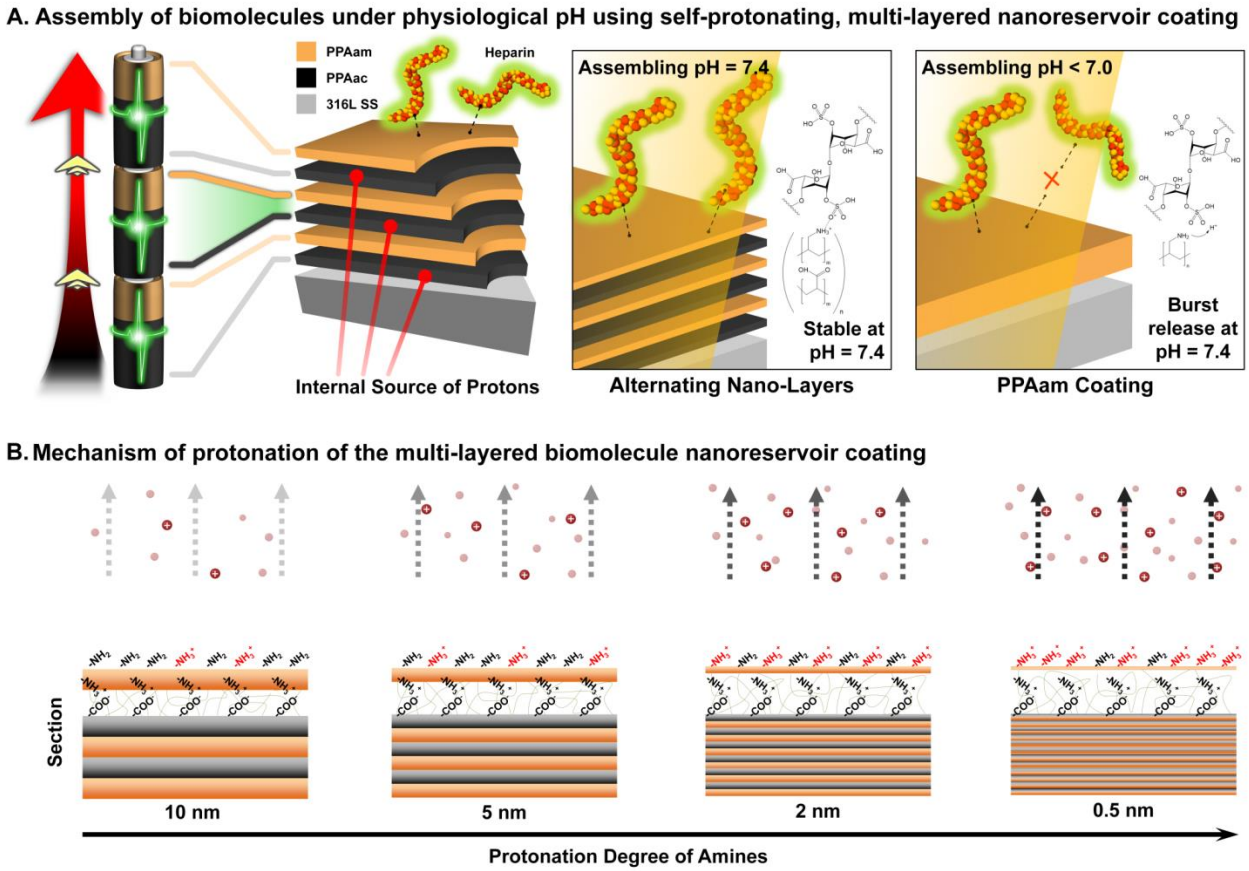

Figure 1. (A) Assembly of biomolecules under physiological pH using highly self-protonating, multi-layered nanoreservoir coating. Upon plasma polymerization, acrylic acid/allylamine (PPAam/Aac) nanolayers form electrostatic complex with many interacting layers through strong voltage and ionic interactions, mimicking the redox surfaces of a typical power cell to generate high potential difference compared to singular coatings for secure conjugation of biomolecules under physiological pH; whereas assembly of traditional layer-by-layer deposition relies solely on positive charges generated from acidic environments (excess H^+), which eventually dissipates under physiological conditions (neutralized H^+). (B) Mechanism of protonation of the multi-layered biomolecule nanoreservoir coating, where the top-most layers of the coatings are zoomed in for clarity. Under identical nominal thickness, protonation degree of amines increases with the

number of interacting layers (3-60). By reducing the layer thickness from 10 nm to 0.5 nm, more PPAam-PPAac interacting layers and thus potential difference are created, generating a stronger proton updraft to the surface from the reservoir for conjugation of biomolecules.

Results and discussion

1. Fabrication and characterization of *in situ* self-protonating coatings

To determine the optimal coating ratios, we fabricated four *in situ* self-protonating coatings (PPAam/Aac) of identical nominal thickness (60 nm) but varied monolayer thicknesses (0.5, 2, 5 and 10 nm) on mirror-polished stainless steel using plasma polymerization: inductively coupled plasma was excited by external copper band electrodes with a 13.56 MHz pulsed radio frequency (RF) [6]. 60 nm is selected as this coating thickness can resist abrasion and wear, with no detrimental effects on lumen size for prevention of occlusion, while maintaining decent charge potency [9]. By spectroscopic ellipsometer, the actual film thickness was determined to be 60 – 66 nm for all groups **(Figure S1 and Table S1)**. We used X-ray photoelectron spectroscopy (XPS) to determine the chemical composition and surface protonation degree of our coatings, and verified significantly different C/N/O composition ratios in alternating coatings compared to pure PPAam and PPAac **(Table S2)**. We further investigated the relation between the nanolayer thickness and the surface amine protonation degree using high-resolution N1s spectra of XPS **(Figure 2A)**, and discovered a gradual increase of $R–NH_3^+$ ratios as individual thicknesses decrease (9.1% to 20.9%). This suggests that increased layer density leading to improved redox potential of interfaces can achieve a stronger longitudinal migration of protons upwards in favor of protonation at the surface. Other than surface charge potential, these protonated amine groups also contribute to hydrophilicity (increasing hydrophilicity with decreasing thickness, **Figure**

S2A), and improve the overall coating biocompatibility. To assess the surface charge for biomolecule conjugation, we further quantified primary amine (-NH_2) and carboxylic groups (-COOH) using 4-trifluoromethylbenzaldehyde (TFBA) derivatization and Toluidine blue-O (TBO) methods on the coating surface, which showed reduced -NH_2 and increased -COOH exposure with decreasing thickness **(Figure 2B and 2C)**. This demonstrates that the extreme thinness of nanolayers may cause incomplete coverage of PPAam, leading to "holes" on nanolayers and non-homogeneity in topmost layers. We further reinforce this idea by measuring zeta-potential of nanolayer coatings. As expected, zeta-potential of the PPAam/Aac-10 nm and PPAam/Aac-5 nm coatings was higher than the pure PPAam and increases with layer density **(Figure S2B).** The positive charge, however, showed a surprisingly sharp decrease starting at 2 nm layer thickness. This may be attributed to the technical limitations of plasma polymerization: overly short reaction times may lead to incomplete polymerization, causing a possible dissolution of plasma polymer fragments and mixed exposure of both -NH_2 and -COOH groups when immersed, leading to a decline of zeta potential despite the high R–NH_3^+ ratios [10]. Henceforth, there exists a delicate but realistic balance between the protonating efficacy and surface charge density to achieve optimal biomolecule conjugation efficacy, of which we must fine-tune via controlling individual layer thickness going forward.

2. Loading efficiency of heparin onto *in situ* self-protonating coatings

We then evaluated the performance of the above fabricated *in situ* self-protonating PPAam/Aac surfaces in stabilizing biomolecules. We selected heparin as the model biomolecule due to its anti-coagulant property and popularity to modify vascular devices and performed its conjugation via simple dipping/washing [11]. To examine the heparin immobilization capacity of our system

in a static environment, we first incubated the coated substrates in 1 mg/mL heparin (sodium salt, potency > 150 U/mg, Sigma) phosphate buffer saline (PBS) solution at pH 7.4 for 2 h, followed by washing with distilled water 3 times for 15 min. We measured the adsorption and retention of heparin using sulphur signals from XPS. We demonstrated its successful binding via electrostatic interactions between $-SO_3^{2-}$ of heparin and $-NH_3^+$ of PPAam through the presence of sulphur (S2p) peaks **(Figure 2D)**. We then quantified the amount of adsorbed heparin through Scofield Sensitivity Factors based on sulfur content **(Figure 2E)**. Interestingly, the highest heparin binding does not belong to the highest surface $-NH_3^+$ concentration (highest in PPAam/Aac-0.5 nm) nor the highest zeta potential (highest in PPAam/Aac-5 nm) **(Figure S2A, S2B)**. Instead, PPAam/Aac-2 nm group showed the most heparin binding, supporting our hypothesis of equilibrium between the zeta potential and the protonating efficacy in our alternating nanolayer coating, where 2 nm is the thinnest layer thickness we achieved without sacrificing multilayer integrity.

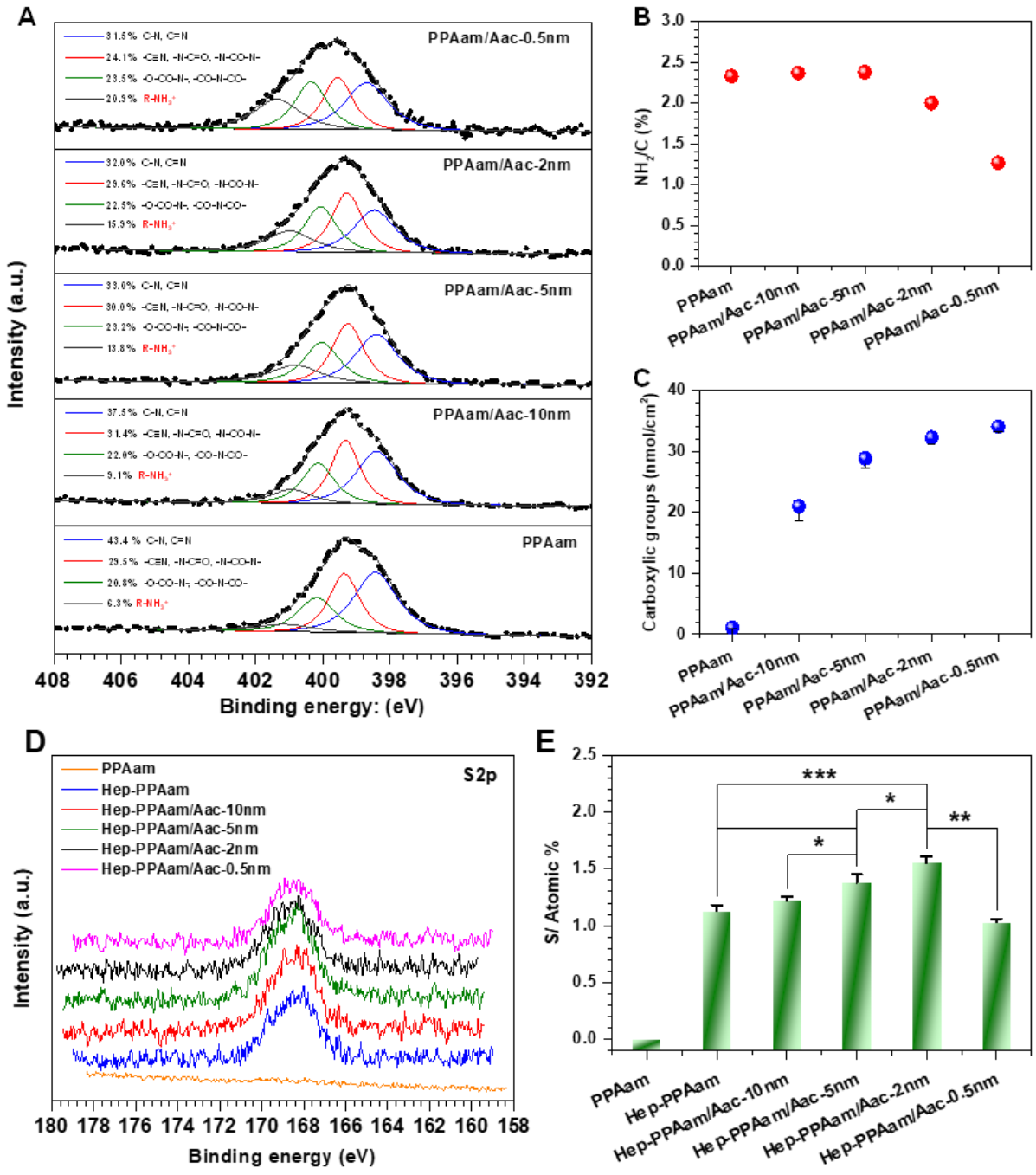

Figure 2. Characteristics of non- and heparinized self-protonating, plasma polymerized, superimposed multi-layered nanoreservoir coatings. (A) High-resolution N1s XPS spectra of plasma polymerized coatings; (B) The primary amine quantification (red plots) and (C) The density of carboxylic groups (blue plots) on surfaces of different coatings. (D) High-resolution

sulfur (S2p) XPS spectra and (E) relative amount of heparin retained on PPAam and *in situ* self-protonating coatings after heparin immobilization. (amount of heparin is represented by S atomic%). Data are presented as mean ± SD and analyzed by one-way ANOVA (n = 4, *p < 0.05, **p < 0.01 and ***p < 0.001).

We further quantified the amount of heparin conjugated under dynamic flow and retained under washing to mimic the native vascular fluid mechanics. While the quantity of heparin was monitored by Quartz Crystal Microbalance with Dissipation monitoring (QCM-D), we immobilized heparin onto the *in situ* self-protonating coatings by injecting 1 mg/mL of heparin dissolved in PBS solution at a rate of 50 μL/min until the QCM-D traces maintained steady, followed by washing with PBS at the same fluid velocity to remove the non-conjugated molecules **(Figure 3A-E)**. We found that the PPAam/Aac-2 nm coating presented landmark performance with the maximum binding amount (509.3 ng/cm^2) and robust binding strength, with no visible burst release or negligible mass change (~5%) under dynamic and high salt (namely ionic strength) flow condition **(Figure 3F)**. This proves that our coated heparin possesses enough robustness to withstand continuous flow conditions which resemble the native never-ending blood flow. Additionally, heparinized coatings were immersed in rabbit serum for 7 days, and activated partial thromboplastin time (APTT) was performed to quantify the relative amount of heparin retained on the surfaces of PPAam, PPAam/Aac-10nm, PPAam/Aac-5nm, PPAam/Aac-2nm, and PPAam/Aac-0.5nm for assessment of long-term stability of heparin **(Figure S3)**. All the alternating multi-layered coating groups exhibited good stability with a small gradual drop in heparin functionality while PPAam exhibited a sharp decrease in heparin amount over 7 days of immersion.

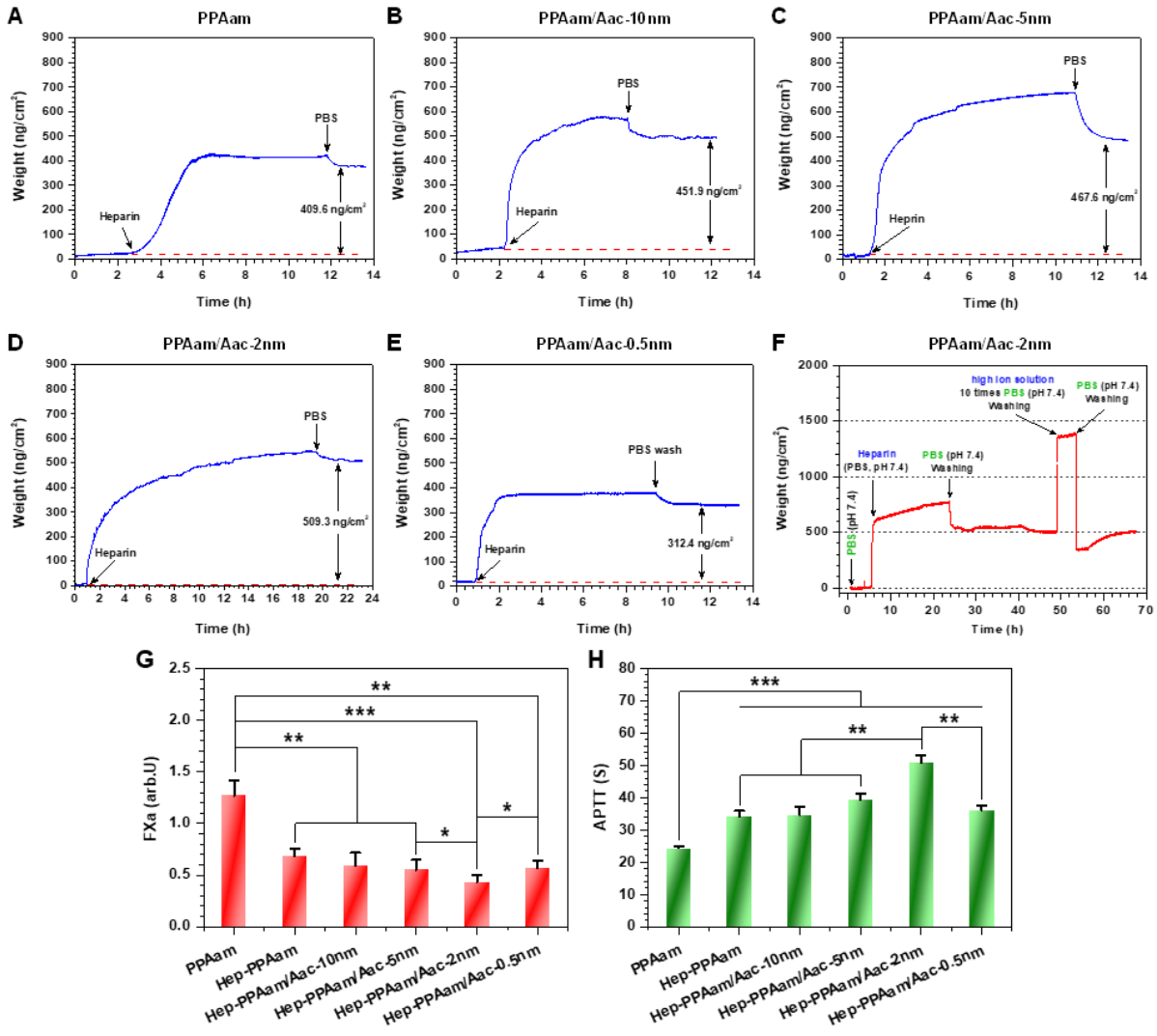

Figure 3. Assembly, stability, and bioactivity of heparin using the self-protonating, plasma polymerized and superimposed multi-layered nanoreservoir coatings. Real-time monitoring of heparin assembly on (A) PPAam, (B) PPAam/Aac-10 nm, (C) PPAam/Aac-5 nm, (D) PPAam/Aac-2 nm and (E) PPAam/Aac-0.5 nm coatings by QCM-D. (F) Stability of the assembled heparin on PPAam/Aac-2 nm coating by extensive washing with both PBS solution and high ion concentration (10X PBS). FXa activity (G) and APTT analysis (H) of different samples. Data are presented as mean ± SD and analyzed by one-way ANOVA (n = 4, *$p < 0.05$, **$p < 0.01$ and ***$p < 0.001$).

3. Assessment of *in vitro* bioactivity of heparin-loaded *in situ* self-protonating coatings

With heparin securely conjugated onto our nanolayer coating, we then move onto assessing heparin bioactivity after assembly both *in vivo* and *ex vivo* since loss of biomolecule activity (e.g., change of biomolecule structural conformation) is a major concern in traditional immobilization methods. Firstly, we performed hemolysis and cell proliferation to assess our nanolayer coating's biocompatibility and stability. The hemolysis ratios of all plasma-polymerized film modified samples were shown to be within 1%, demonstrating their hemocompatibility **(Figure S4)**, while no significant differences could be observed in proliferation of human umbilical vein cells (HUVECs) between different sample groups **(Figure S5)**. Next, we performed the anti-Factor Xa (anti-FXa) activity test and the activated partial thromboplastin time (APTT) test using chromogenic anti-FXa assay (bovine FXa, COAMATIC® Heparin) [12-14]. Compared to pure PPAam coating, the heparinized surfaces had significantly higher anti-FXa activity. The PPAam/Aac-2 nm showed the highest value of ~3.0 folds compared to the pure PPAam coating, indicating the remarkably increased anti-FXa activity and anti-thrombin III (ATIII) activity (**Figure 3G**). On the other hand, APTT test showed a direct correlation between the APTT and the amount of immobilized heparin by measuring the time required to form blood clots (**Figure 3H**). As the coating with highest conjugated heparin, PPAam/Aac-2 nm was able to sustain about 2.1 folds longer APTT time than the pure PPAam, demonstrating the excellent retention of anti-coagulant activity of conjugated heparin of our self-protonating PPAam/Aac coatings.

As known, heparin improves hemocompatibility when being used in vascular device coatings due to its suppression of fibrinogen (Fg) and subsequently platelet activation [11, 15]. Hence, we evaluated the adsorption and activation of Fg, as well as the platelet adhesion and activation onto our coatings after incubation in platelet poor plasma (PPP) as another assessment

for heparin bioactivity. We found that both the Fg adsorption and activation on the heparinized surfaces were significantly lower than the pure PPAam surface **(Figure 4A-i and ii)**. We also observed platelet morphology on our coatings using scanning electron microscope (SEM), which showed most platelets on pure PPAam fully spread out, indicating a highly activated state whereas on the heparin immobilized surfaces, most adherent platelets maintained a round shape, suggesting a resting and non-activated state **(Figure 4B-i)**. This is further supported by similar results from P-selectin staining of platelets **(Figure S6)**, with pure PPAam having 6.6 folds of activated platelets compared to PPAam/Aac-2 nm. These results combined indicate the robust retention of heparin bioactivity under *in vitro* conditions, which allows for effective inhibition of platelets and fibrin and prevention of post-implantation thrombosis.

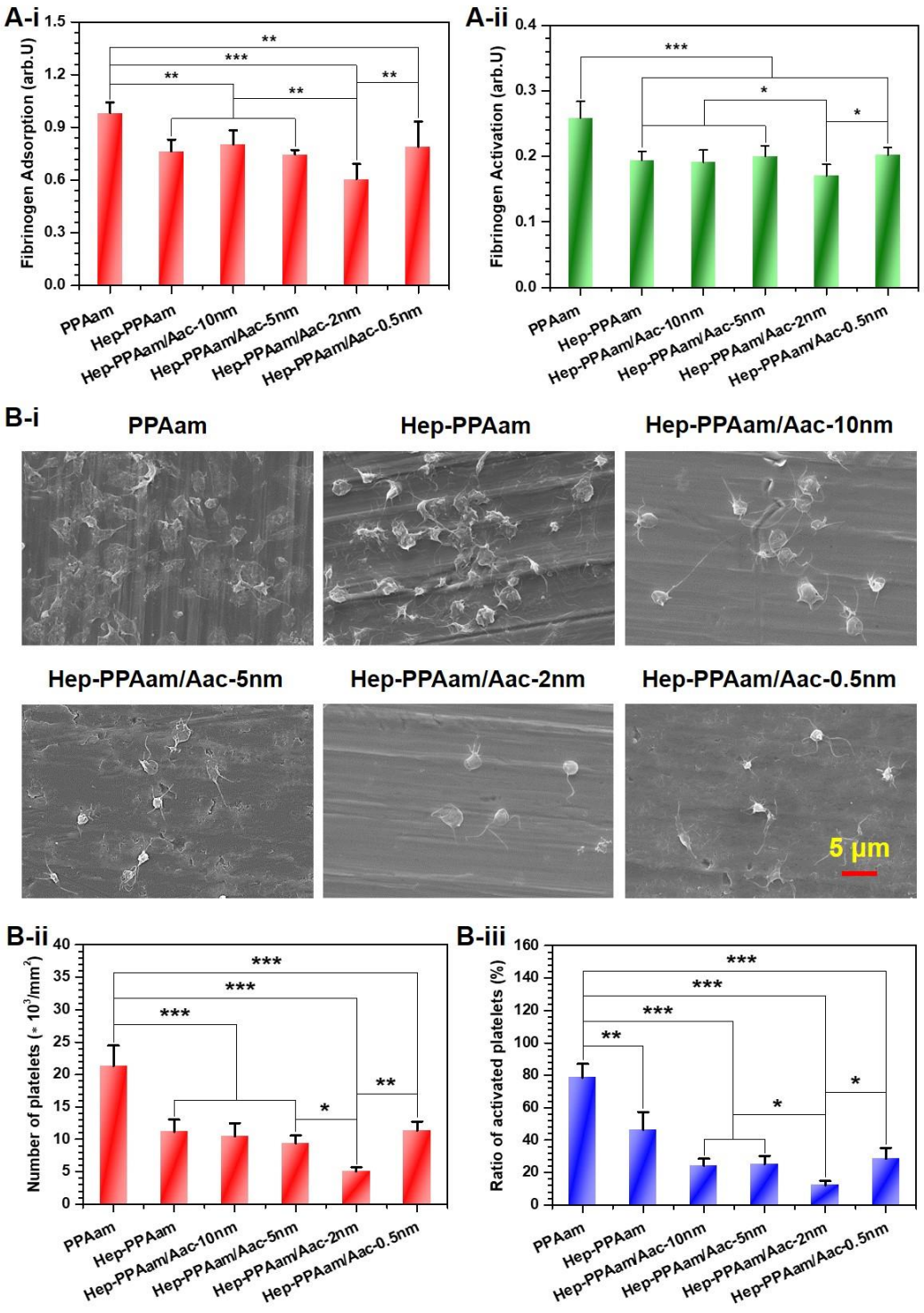

Figure 4. *In vitro* anti-coagulation property of the self-protonating, plasma polymerized and superimposed multi-layered nanoreservoir coatings. (A-i) Fibrinogen adsorption and (A-ii) activation on different heparinized self-protonating samples. (B-i) Morphology of platelets

adhered on the surfaces of various samples observed using SEM; (B-ii) The number of the adhered platelets and (B-iii) the ratio of the activated platelets on different samples (the size of sample: 1 cm × 1 cm, n = 4) were calculated from at least 6 random SEM images. Data are presented as mean ± SD and analyzed by one-way ANOVA (n = 4, *p < 0.05, **p < 0.01 and ***p < 0.001).

4. Assessment of *ex vivo* bioactivity of heparin-loaded *in situ* self-protonating coatings

While simulation of improved hemocompatibility was observed in *in vitro* assessments of the heparin modified PPAam/Aac surfaces, their clinical relevance greatly depends on whether the biomolecules would persist while in contact with native blood circulation. To further examine the anti-thrombogenic properties of the heparin modified PPAam/Aac surfaces in actual blood circulation, we implemented an *ex vivo* blood circulation experiment by assembling pure PPAam and heparin-modified 316L stainless steel foils into polyvinyl chloride (PVC) tubes connecting the left carotid artery and the right external jugular vein of a rabbit **(Figure 5A)**. We observed that only minor clotting can be found on the heparin-modified samples while massive thrombus formed on pure PPAam surface **(Figure 5B)**. Besides, the PPAam surface evoked severe thrombus formation and led to complete occlusion, while all heparin-coated foils were not obstructed **(Figure 5C)**. Notably, the PPAam/Aac-2 nm surface had the lowest occlusion rate (10.4%, 9.9 folds lower than control), smallest obtained thrombus weight (6.9 mg, 15.3 folds lower than control) and the highest blood flow rate (97.2%, 34.5-fold increase compared to control) **(Figure 5D-F)**, indicating that the anti-coagulant effect was highly associated with the amount of heparin immobilized on the PPAam/Aac surfaces. Coupled with the excellent hemocompatibility *ex vivo*, we could conclude that our *in situ* self-protonating PPAam/Aac

coating strategy was largely successful at conjugating heparin onto blood-contacting devices' surfaces and maintaining its structural integrity and bioactivity.

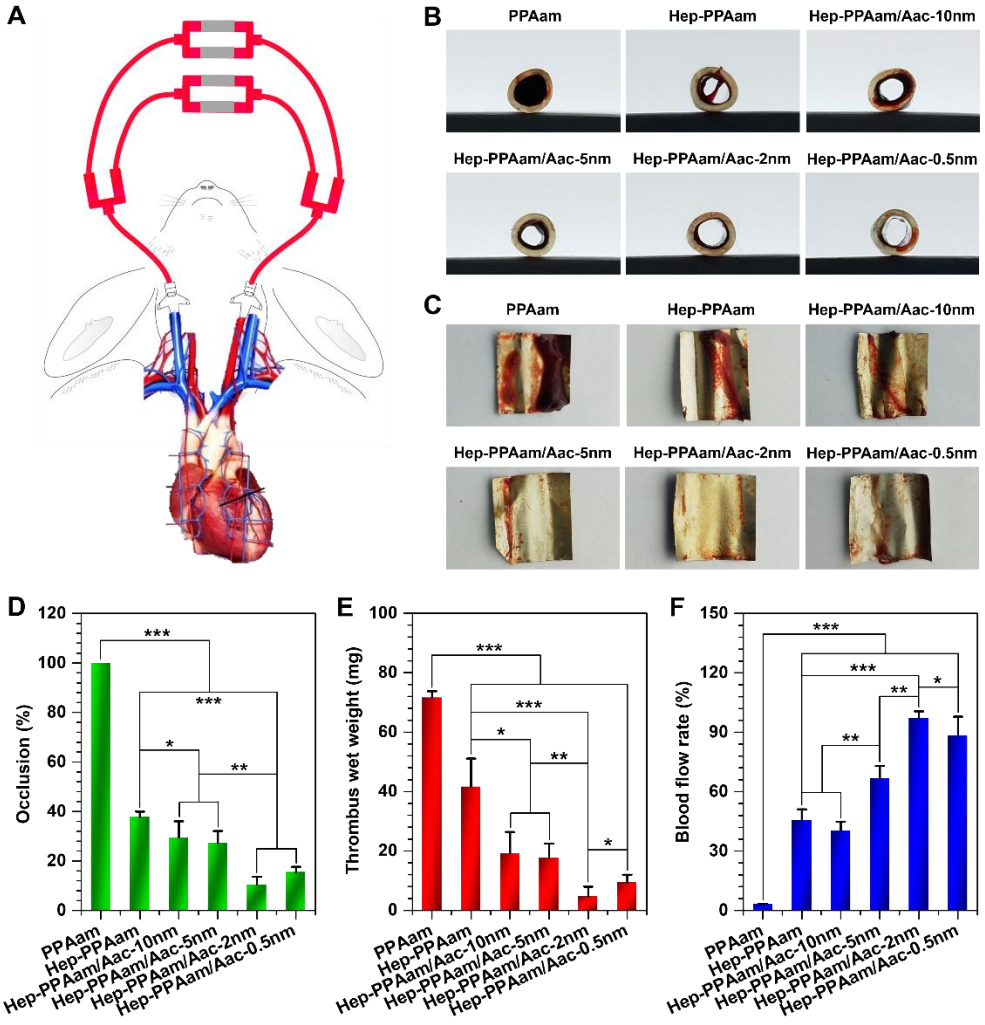

Figure 5. *Ex vivo* anti-coagulation properties of the self-protonating, plasma polymerized and superimposed multi-layered nanoreservoir coatings to illustrate its clinical potential for improving hemocompatibility in blood-contacting devices. (A) Schematic depicting the *ex vivo* experimental set up of New Zealand Rabbit arteriovenous (AV) shunt models, where polyvinyl chloride (PVC) tubes containing modified 316L stainless steel foils connect the left carotid artery and the right external jugular vein for assessment of anti-thrombogenic properties. Photographs of (B) formed thrombus in cross-section view of curled foils and (C) flattened view of

intersecting surfaces of different surface-modified foils after 2 h of blood flow. (D) Percentage occlusion of circuits and (E) thrombus weight and (F) blood flow rate of different samples after 2 h of blood flow. Data are presented as mean ± SD and analyzed by one-way ANOVA (n = 4, *p < 0.05, **p < 0.01 and ***p < 0.001).

Conclusion

The prime objective of device coatings is to shield foreign substances from contacting native cells and triggering complications. The advancement in plasma technology has allowed for non-thermal polymerization to create coatings with vast possibilities to be functionalized with biological cues for controlling cell behavior [16, 17]. While other studies may utilize strong acid treatment for conjugation of molecules, risking leaching of metal ions and corrosion, our coating system, however, utilizes plasma-sprayed nanolayers of polymers to first create charged surfaces for adhesion of biomolecules, which simultaneously protects devices from erosion [18]. To achieve effective shielding, robustness of both coating itself and its conjugated biomolecules are of equal importance. Overall smoothness can greatly reduce friction and wear of surface molecules, which is especially crucial in blood-contacting devices, where drug-eluting coatings often lose their anti-coagulant molecules too quickly and cause thrombosis due to the surface roughness of coating [19]. This also potentially explains the excellent retention of biomolecules even under dynamic flow conditions in our system due to the lowered frictional drag in proximity of coating [20]. Another attribute is the highly condensed charge potential of PPAam/Aac nanolayers. It has been demonstrated by cyclic voltammograms of PPAam/Aac that addition of each bilayers can gradually raise a system's electroactivity [21]. In our best performing nanolayer coating, PPAam/Aac-2 nm, 15 interfaces were generated, which greatly

boasts its electrical potential and surface charge for biomolecule adhesion. Moreover, coating systems are gradually evolving towards solving problems created by surgical procedures. For example, recovery from damaged endothelium in stenting can be accelerated through integrating nitric oxide precursors and vascular endothelial growth factor (VEGF) in stent coatings [6, 11, 22-25]. This in turn greatly raises the requirements of bioactivity retention in biomolecular coating systems since regenerative molecules such as growth factors are more fragile, and would not be able to survive in slightly acidic pHs even at 5-6, thus creating a need for green fabrication strategies. Our self-protonating, plasma polymerized, superimposed multi-layered nanoreservoir coating strategy can conjugate any charged biomolecules at physiological pHs with unprecedented robustness and bioactivity retention, and we envision this technique to be able to revolutionize the clinical device coating field with its green fabrication, anti-scratch flow resistance and reliable loading of biomolecules.

Supporting Information

Supplementary table and figures, with detailed description of experimental methods (PDF)

Conflict of interest statement

The authors declare that there is no conflict of interest. Wenxuan Wang, Lei Lu and Ho Pan Bei contributed equally to this manuscript.

Acknowledgment

This work was supported by the Innovation and Technology Fund (ITS/065/19) from The Hong Kong Innovation and Technology Commission (ITC), the National Natural Science Foundation of China (31570957, 31800795), the National Key Research and Development Program of China (2017YFB0702504), the International Cooperation Project by Science and Technology Department of Sichuan Province (2019YFH0103) and the Applied Basic Research Project funded by Sichuan Provincial Science and Technology Department (2017JY0296). We would also like to thank the Analytical and Testing Center of Southwest Jiaotong University for the SEM test.

References

[1] L.M. Szott, C.A. Irvin, M. Trollsas, S. Hossainy, B.D. Ratner, Blood compatibility assessment of polymers used in drug eluting stent coatings, Biointerphases 11 (2016) 029806.

[2] Z. Yang, X. Zhao, R. Hao, Q. Tu, X. Tian, Y. Xiao, K. Xiong, M. Wang, Y. Feng, N. Huang, Bioclickable and mussel adhesive peptide mimics for engineering vascular stent surfaces, Proc. Natl. Acad. Sci. U.S.A. 117 (2020) 16127-16137.

[3] Y. Hou, X. Deng, C. Xie, Biomaterial surface modification for underwater adhesion, Smart Materials in Medicine (2020).

[4] B.R. Coad, M. Jasieniak, S.S. Griesser, H.J. Griesser, Controlled covalent surface immobilisation of proteins and peptides using plasma methods, Surf. Coat. Technol. 233 (2013) 169-177.

[5] S. Ayati Najafabadi, H. Keshvari, Y. Ganji, M. Tahriri, M. Ashuri, Chitosan/heparin surface modified polyacrylic acid grafted polyurethane film by two step plasma treatment, Surf. Eng. 28 (2012) 710-714.

[6] T. Yang, Z. Du, H. Qiu, P. Gao, X. Zhao, H. Wang, Q. Tu, K. Xiong, N. Huang, Z. Yang, From surface to bulk modification: Plasma polymerization of amine-bearing coating by synergic strategy of biomolecule grafting and nitric oxide loading, Bioact. Mater 5 (2020) 17-25.

[7] Z. Zhang, G. Li, F. Yan, X. Zheng, X. Li, Towards understanding of protein adsorption behavior on plasma polymerized pyrrole film, Open Chem. J. 10 (2012) 1157-1164.

[8] J. Chen, N. Huang, Q. Li, C.H. Chu, J. Li, M.F. Maitz, The effect of electrostatic heparin/collagen layer-by-layer coating degradation on the biocompatibility, Appl. Surf. Sci. 362 (2016) 281-289.

[9] F.F. Conde, J.A.Á. Diaz, G.F.d. Silva, A.P. Tschiptschin, Dependence of wear and mechanical behavior of nitrocarburized/CrN/DLC layer on film thickness, Mater. Res. 22 (2019).
[10] P. Gao, H. Qiu, K. Xiong, X. Li, Q. Tu, H. Wang, N. Lyu, X. Chen, N. Huang, Z. Yang, Metal-catechol-(amine) networks for surface synergistic catalytic modification: Therapeutic gas generation and biomolecule grafting, Biomaterials (2020) 119981.
[11] Y. Yang, P. Gao, J. Wang, Q. Tu, L. Bai, K. Xiong, H. Qiu, X. Zhao, M.F. Maitz, H. Wang, Endothelium-Mimicking Multifunctional Coating Modified Cardiovascular Stents via a Stepwise Metal-Catechol-(Amine) Surface Engineering Strategy, Research 2020 (2020) 9203906.
[12] Z. Yang, Q. Tu, M.F. Maitz, S. Zhou, J. Wang, N. Huang, Direct thrombin inhibitor-bivalirudin functionalized plasma polymerized allylamine coating for improved biocompatibility of vascular devices, Biomaterials 33 (2012) 7959-7971.
[13] L. Lu, Q.L. Li, M.F. Maitz, J.L. Chen, N. Huang, Immobilization of the direct thrombin inhibitor-bivalirudin on 316L stainless steel via polydopamine and the resulting effects on hemocompatibility in vitro, J Biomed Mater Res A 100 (2012) 2421-2430.
[14] K.N. Sask, I. Zhitomirsky, L.R. Berry, A.K. Chan, J.L. Brash, Surface modification with an antithrombin–heparin complex for anticoagulation: studies on a model surface with gold as substrate, Acta Biomater 6 (2010) 2911-2919.
[15] Z. Wang, W. Sun, Z. Wei, J. Bao, X. Song, Y. Li, H. Ji, J. Zhang, C. He, B. Su, Selective potassium uptake via biocompatible zeolite–polymer hybrid microbeads as promising binders for hyperkalemia, Bioact. Mater 6 (2020) 543-558.
[16] T. Egghe, P. Cools, J.F. Van Guyse, M. Asadian, D. Khalenkow, A. Nikiforov, H. Declercq, A.G. Skirtach, R. Morent, R. Hoogenboom, Water-Stable Plasma-Polymerized N, N-

Dimethylacrylamide Coatings to Control Cellular Adhesion, ACS Appl. Mater. Interfaces 12 (2019) 2116-2128.

[17] L. Gao, X. Shi, X. Wu, Applications and challenges of low temperature plasma in pharmaceutical field, J. Pharm. Anal (2020).

[18] M. Keeney, M. Mathur, E. Cheng, X. Tong, F. Yang, Effects of polymer end-group chemistry and order of deposition on controlled protein delivery from layer-by-layer assembly, Biomacromolecules 14 (2013) 794-800.

[19] T.M. Bedair, Y. Cho, B.J. Park, Y.K. Joung, D.K. Han, Coating defects in polymer-coated drug-eluting stents, Biomater. Biomed. Eng 1 (2014) 131.

[20] Y. Chen, Y. Xiong, W. Jiang, M.S. Wong, F. Yan, Q. Wang, Y. Fan, Numerical simulation on the effects of drug-eluting stents with different bending angles on hemodynamics and drug distribution, Med Biol Eng Comput 54 (2016) 1859-1870.

[21] Z. Hu, J. Xu, Y. Tian, R. Peng, Y. Xian, Q. Ran, L. Jin, Layer-by-layer assembly of polyaniline nanofibers/poly (acrylic acid) multilayer film and electrochemical sensing, Electrochim. Acta 54 (2009) 4056-4061.

[22] R. Hou, L. Wu, J. Wang, Z. Yang, Q. Tu, X. Zhang, N. Huang, Surface-Degradable Drug-Eluting Stent with Anticoagulation, Antiproliferation, and Endothelialization Functions, Biomolecules 9 (2019) 69.

[23] Z. Yang, Y. Yang, L. Zhang, K. Xiong, X. Li, F. Zhang, J. Wang, X. Zhao, N. Huang, Mussel-inspired catalytic selenocystamine-dopamine coatings for long-term generation of therapeutic gas on cardiovascular stents, Biomaterials 178 (2018) 1-10.

[24] Q. Tu, X. Zhao, S. Liu, X. Li, Q. Zhang, H. Yu, K. Xiong, N. Huang, Z. Yang, Spatiotemporal dual-delivery of therapeutic gas and growth factor for prevention of vascular stent thrombosis and restenosis, Appl. Mater. Today 19 (2020) 100546.

[25] Q. Tu, X. Shen, Y. Liu, Q. Zhang, X. Zhao, M.F. Maitz, T. Liu, H. Qiu, J. Wang, N. Huang, A facile metal–phenolic–amine strategy for dual-functionalization of blood-contacting devices with antibacterial and anticoagulant properties, Mater. Chem. Front 3 (2019) 265-275.